The Pennsylvania State University

The Graduate School

College of Medicine

TARGETED LIPOSOMES FOR TREATMENT OF ALS IN MUTANT SOD1^{G93A} MOUSE MODEL

A Thesis in

Neuroscience

by

Nicholas J. Wiley

Submitted in Partial Fulfillment
of the Requirements
for the Degree of

Master of Science

August 2008

The thesis of Nicholas J. Wiley was reviewed and approved* by the following:

James R. Connor
Distinguished Professor and Vice-Chair Department of Neurosurgery
Thesis Adviser

Robert J. Milner
Program Director of Neuroscience
Professor of Neural and Behavioral Sciences

Zachary Simmons
Professor of Neurology

*Signatures are on file in the Graduate School.

ABSTRACT

Amyotrophic lateral sclerosis (ALS) is a rapidly progressive and fatal neurological disease characterized by the selective death of motor neurons. There is substantial evidence that degeneration is propagated by activated microglia and accompanying inflammation. To this end, several therapeutic agents have aimed to curb microglia activation, albeit with little success. The present study aimed to increase site-specific concentration and thus drug efficacy with the use of an osmotic intracerebroventricular (ICV) pump by delivering minocycline contained in liposomes with a targeting moiety specific to microglial cell surface markers. It was hypothesized that attenuating microglial activation would delay the kinetics of disease progression. The potential therapeutic efficacy of this approach was shown in both *in vitro* models with mouse microglia-derived BV-2 cells as well as an *in vivo* model involving mutant $SOD1^{G93A}$ mice. The *in vitro* results indicate that targeting the TLR4/LPS complex significantly increases ($p<0.05$) the uptake of drug by 29% compared to non-targeted liposomes. In the $SOD1^{G93A}$ mouse model of ALS, both targeted and non-targeted minocycline treatment significantly increased ($p<0.05$) latency to endpoint stages compared to control mice receiving no treatment. Although, targeting treatment to microglia only slowed later disease progression with statistical significance. The results of this study provide evidence for a greater role of microglia in disease progression, and not disease onset, and suggests targeting microglia provides a viable therapeutic target for slowing progression after initial clinical diagnosis.

TABLE OF CONTENTS

LIST OF TABLES

LIST OF FIGURES

ACKNOWLEDGEMENTS

This thesis was made possible with the help and technical support of Ryan Mitchell, Logan Douds, Elias Rizk, Madhan Kumar, Beth Neely, and the Connor Laboratory of the Department of Neurosurgery at Pennsylvania State University. A special thanks to my advisor and mentor, Dr. Jim Connor, who challenged and encouraged me throughout my graduate school career.

This work was supported by funds from The Paul and Harriett Campbell Fund for ALS Research and The Zimmerman Family Love Fund.

INTRODUCTION

Amyotrophic lateral sclerosis (ALS) is a neurodegenerative disease hallmarked by the selective death of motor neurons. It was first described in scientific literature in 1869 by the French neurologist Jean-Martin Charcot (Charcot and Joffrey, 1869; Rowland, 2001). The disease name confers its clinical pathology: "a" = no, "myo" = muscle, "trophic" = nourishment, thus no muscle nourishment which causes atrophy to motor neurons in the "lateral" spinal cord, eventually leading to scarring, or "sclerosis". In most individuals with ALS, this results in respiratory depression from loss of diaphragmatic function in about 3-5 years after onset of symptoms (Gubbay et al, 1985). ALS is one of the most common motor neuron diseases with a worldwide incidence of ~1.5-2.5/100,000 individuals per year (Worms, 2001). In addition, the affliction rate is higher among those in their middle age and in men, with a gender ratio of roughly 1.5/1 (Ringel et al, 1993). While the exact etiology of ALS is largely unknown, 90 percent of ALS cases are sporadic in nature with the remaining 10 percent linked to genetic origins (known as familial ALS). Of the latter, a mutation of Cu/Zn superoxide dismutase (SOD1) has been implicated in approximately 20 percent of cases (Rosen et al, 1993). To this end, a transgenic mouse model expressing mutant SOD1 has become a central tool in studying the disease.

SOD1 and the Role of Microglia

Mice with the SOD1 mutation exhibit similar ALS symptomology, which is characterized by leg weakness spreading to the upper limbs and bulbar muscles and eventually causing total paralysis. However, it is still not exactly understood how mutant

SOD1 exerts toxicity to motor neurons. Gurney and colleagues (1994) were the first to report the effects of mutant human $SOD1^{G93A}$ in transgenic mice. In this paper, they also showed that there was an elevated level of SOD1 activity, which provided the foundation that SOD1-associated ALS is the result of a toxic gain of function. This theory was corroborated in several subsequent and independent studies. The first study showed that $SOD1^{G37R}$ mice developed ALS symptomology despite a conservation of free radical scavenging, suggesting that the murine motor neuron disease was the result of mutant SOD1 toxicity and not from a lack of enzymatic activity (Wong et al, 1995). In 1998, Bruijn and colleagues showed that both elimination and elevation of wild-type SOD1 had no effect on mutant-mediated disease onset, and discovered mutant SOD1 protein aggregates to be a common histological feature (Bruijn et al, 1998). Yet another study showed that SOD1 knockout mice failed to develop ALS symptomology (Reaume et al, 1996). These findings all suggest that mutant SOD1 is a toxic gain of function; however, given that SOD1 is a ubiquitously expressed protein, it is still unclear why its toxicity is discriminate to motor neurons. In other words, are activated microglia excreting neurotoxins that is propagating damage to motor neurons and inducing neurodegeneration? Or are neurotoxins and mutant SOD1 accumulation damaging microglia, which results in a loss of their protective function? This question requires a further knowledge of microglia and their purported role in neurodegenerative disorders.

Microglia are the resident immune cells of the central nervous system and account for 10-20 percent of the total glia cell population (del Rio-Hortega, 1958). Microglia are functionally and immunophenotypically related to macrophages in the blood system. During late embryonic and early postnatal maturation of the brain, microglia generally

aid in the clearance of cells undergoing apoptosis, or programmed cell death (Milligan et al, 1991). In the mature brain, resting microglia are characterized by a ramified morphology and are functionally quiescent while serving a central role in immune surveillance. As such, microglia are especially sensitive to changes in the CNS microenvironment and rapidly become activated in response to invading pathogens or injury. Activation is accompanied with a drastic change in morphology from a resting ramified to activated amoeboid state, and an upregulation of several pro- and anti-inflammatory soluble factors. The pro-inflammatory signaling cascade complements the phagocytic function of activated microglia and aids in microgliosis, the recruitment of more immune cells. These factors include major histocompatability complexes (MHC-I and MHC-II), co-stimulatory molecules (CD-80 and CD-86), pro-inflammatory cytokines (IL-1, IL-6, IL-12, IL-18 and TNF-α), chemokines (MIP-1α, MIP-1ß, MCP-1, RANTES, and IP-10), reactive oxygen species, proteases, excitatory amino acids, and nitric oxide (Raivich et al, 1996; Kreutzberg, 1996; van Rossum and Hanisch, 2004). Anti-inflammatory cytokines (IL-1ra, IL-10, and TGF-ß) and neurotrophic factors (glia-derived neurotrophins) in turn downregulate the pro-inflammatory cytokine production and promote survival and regeneration of neurons (van Rossum and Hanisch, 2004).

In principle, activation of microglia has a neuroprotective effect of the CNS; however, chronic activation has been implicated in acute and chronic neurodegeneration. This exacerbation of damage by microglia was originally discovered in the histological analysis of the postmortem brains of Alzheimer's patients where reactive microglia had co-localized with neuritic plaques (Rogers et al, 1988) and in Parkinson's patients where reactive microglia were found in the substantia nigra (McGeer et al, 1988). In ALS,

studies have shown that elevation of microglial pro-inflammatory mediators accompany motor neuron loss (Hensley et al, 2003), and that neuronal cell death is associated with inflammation and microgliosis, the combination of which has been shown to have a neurotoxic role in the pathogenesis of the disease (Alexianu et al, 2001; Kawamata et al, 1992). This concept has also been demonstrated in mutant SOD1 mice where microglial activation precedes observable weakness and motor neuron loss, and in studies showing that chronic stimulation of microglia exacerbates the disease (Nguyen et al, 2004). It is widely debated, however, whether activated microglia are involved in the initiation stage of disease progression or occurs in response to neuronal death. Still, the administration of anti-inflammatory compounds to attenuate microglia activation has been widely explored in both *in vitro* and *in vivo* models of neurodegenerative disease.

Minocycline Therapy

The delivery of anti-inflammatory compounds, such as minocycline, has been studied extensively in animal models of ALS as well as other neurodegenerative diseases where activation of microglia is a histological feature. Despite being commercially available for nearly three decades, interest in the neuroprotective effects of minocycline emanated from the finding that the drug significantly reduced infarct volume and neuronal cell loss after induced hypoxic injury in gerbils and rats (Yrjänheikki, 1998; Arvin et al, 2002). Subsequent research with minocycline in various models of acute and chronic neurodegeneration corroborated its neuroprotective effect, and extended them to include traumatic brain and spinal cord injury (Sanchez Mejia et al, 2001; Well et al, 2003), multiple sclerosis (Brundula et al, 2002), Parkinson's disease (Du et al, 2001; Wu et al, 2002; He et al, 2001), Huntington's disease (Chen et al, 2000; Wang et al, 2003),

and ALS (Van Den Bosch et al, 2002; Zhu et al, 2002). Despite promising results in the animal models of ALS, there has been a weak corollary of efficacy for minocycline in human clinical trials. Indeed, a recently published phase III trial of minocycline with ALS patients reported a potential harmful effect (Gordon et al, 2007). Possible explanations for this effect are the inadvertent toxicity of motor neurons due to nonselective oral drug administration or the inability to deliver sufficient amounts of drug to where it is needed, both problems that may be circumvented via a targeting drug delivery system and/or by direct infusion into the lateral ventricles of the cerebral cortex.

Targeted Drug Delivery Systems

As previously mentioned, one of the disadvantages of most systemically-delivered drugs is that they exert their biological effects not only at their target sites but also at peripheral tissue and cells. This often results in undesired side effects and greatly reduces the therapeutic potential of the drug. The ultimate goal of drug delivery systems is to avoid this by selectively targeting pathological sites. To this end, liposomal drug carriers have shown much promise.

Liposomes were first described in literature by Bangham and Horne (1964) when it was discovered that a negative stain added to dry phospholipids resulted in a plasmalemma, or phospholipid bilayer, able to be visualized by an electron microscope. Subsequent research demonstrated that hydrophobic compounds can be incorporated into the phospholipid bilayer, and hydrophilic drugs could be encapsulated in the inner aqueous compartment of liposomes (Johnson et al, 1971; Bangham, 1972; Gregoriadis et al, 1974). However, one of the innate problems with first generation liposomes was the fast clearance of the nanovesicles in the bloodstream by the reticuloendothelial system

(Segal et al, 1974). Thus virtually all liposomes today are coated with a hydrophilic polymer, such as poly(ethylene glycol), to provide steric stabilization to the liposomes and to significantly increase their circulating half-life (Morgan et al, 1983).

The first liposome drug product to be commercialized was a pegylated liposomal doxorubicin under the trade name Doxil® (Caelyx® in the European Union). The *in vivo* pharmacokinetic studies of Doxil revealed that the area under the curve (AUC, plasma concentration by time) after a dose of 50 mg/m^2 is approximately 300-fold greater than that with free drug (Rahman et al, 1990; Gabizon et al, 2003), while there was a 6-fold increase in the AUC for tumor uptake (Vaage et al, 1997). This contrast in plasma AUC and tumor AUC may be explained by the fact that Doxil relies on passive liposome targeting. In other words, Doxil is effectively taken up because of the natural leaky vasculature of the tumor and accumulation a result of the limited drainage (Hashizume et al, 2000). In contrast, active liposomal targeting strategies have been developed wherein ligands are conjugated to the liposome to actively target specific cells through a ligand-receptor interaction and subsequent internalization of the drug-loaded vehicles. An example of the therapeutic benefit of active targeting is seen with doxorubicin loaded liposomes conjugated with interleukin-13 (IL-13). Due to the high specificity of IL-13 to the IL-13Rα2 receptor on multiforme gliobastromas, researchers have been able to efficiently target therapeutics and significantly reduce tumor size as compared to non-targeted liposomes or conventional free drug administration (Madhankumar et al, 2006). While targeted liposomal drug delivery systems are becoming increasingly more prevalent in the literature, to our knowledge the use of a targeted liposome with specificity for microglia, as presented in this paper, has not been previously shown. As

such, our central hypothesis is that minocycline contained in liposomes and delivered ICV will delay disease onset and increase lifespan in mice carrying the Cu/Zn superoxide dismutase-1 mutation (mSOD1) as compared to control mSOD1 mice receiving no treatment. Our secondary hypothesis is that liposomes targeted to microglia are more effective than non-targeted nanovesicles because of the increased drug specificity and reduction of secondary damage by downstream inflammatory effectors. Finally, the broad, long-term objective for this research is to develop a targeted nanotechnology platform that will improve treatment options for individuals suffering from ALS.

MATERIALS AND METHODS

Preparation and Characterization of Liposomes

Sterically stable liposomes were formulated from dipalmitoylphosphatidylcholine, cholesterol, and 1,2-distearoyl-sn-glycero-3-phosphoethanolamine-N-[carboxy(polyethylene-glycol)2000 purchased from Avanti Lipids (Alabaster, AL), with a molar ratio of 10:2.5:1.5, respectively. The lipid constituents were dissolved in a methanol/t-butanol (1:1 v/v) mixture. A 600 µl saturated solution (chloroform:methanol, 1:1 v/v) of lipopolysaccharide (Sigma, St. Louis, Missouri) was then added to the lipid mixture for synthesis of the targeted nanovesicles.

Lipopolysaccharide (LPS) was chosen as the targeting moiety for conjugation to the liposomes because of its high affinity for surface markers on microglia (Chow et al, 1999). The signal-transducing receptor for LPS is Toll-Like Receptor 4 (TLR4), which importantly is not expressed on cortical neurons, astrocytes, or oligodendrocytes (Hoshino et al, 1999; Lehnardt et al, 2002). Binding of this complex initiates an intracellular signaling pathway of the innate immune system, which includes both the neuroprotective and neurotoxic effects of microglia as described above (Lehnardt, 2003; Li et al, 2007).

The non-targeted nanovesicles were formulated in a separate batch, in the same manner, but without the addition of LPS. The lipid mixture was subsequently rotary evaporated to obtain a lipid film, which was further dried by passing nitrogen and then placed in a desiccator. For minocycline encapsulation, the lipid film was hydrated in 1.0

ml of 10 mg/ml concentration of minocyline and sterile phosphate buffered saline (PBS) mixture and then reconstituted in a bath-type sonicator for 5 minutes. This minocycline concentration was chosen because of the solubility limitations of minocycline as well as a consideration of previous *in vivo* studies (Zhu et al, 2002; Zhang et al, 2003; Van Den Bosch et al, 2002). Unilammelar nanovesicles were obtained by extruding the liposomes though a two-stacked polycarbonate membrane with pore size of 0.1 μm, followed by a 0.05 μm polycarbonate membrane using a nitrogen pressure–operated extruder (Lipex extruder, Northern Lipids, Inc., Vancouver, British Columbia, Canada). All extrusions were done at an operating pressure of 300 p.s.i. Liposome size and polydispersity index (PDI) was determined by dynamic light scattering, which was conducted using a Malvern Zetasizer Nano apparatus (Malvern Instruments, Worcestershire, England). Zeta potential of the liposomes was measured via phase analysis light scattering utilizing a ZetaPALS instrument (Brookhaven Instruments, Holtsville, NY). The average liposome size was found to be 129 nm (PDI = 0.101) and 118 nm (PDI = 0.110) for targeted and non-targeted liposomes, respectively (Figure 1). The low PDI clearly indicates a narrow size distribution, and thus good liposome homogeny. Mean zeta potentials were -29 mV for both liposomes, which is an appropriate charge for anionic vehicles (Chonn et al, 1991). The final minocycline concentration in targeted and non-targeted nanovesicles was analyzed by solubilizing an aliquot of nanovesicle in methanol and sonicating them at room temperature for 5 min. This solution of solubilized nanovesicles and minocycline was then injected into a HPLC for quantification of the minocycline (Beckman Coulter, Fullerton, CA) fitted with C_{18} column. The targeted and non-targeted nanovesicles were diluted in PBS to maintain an equal concentration in both.

A

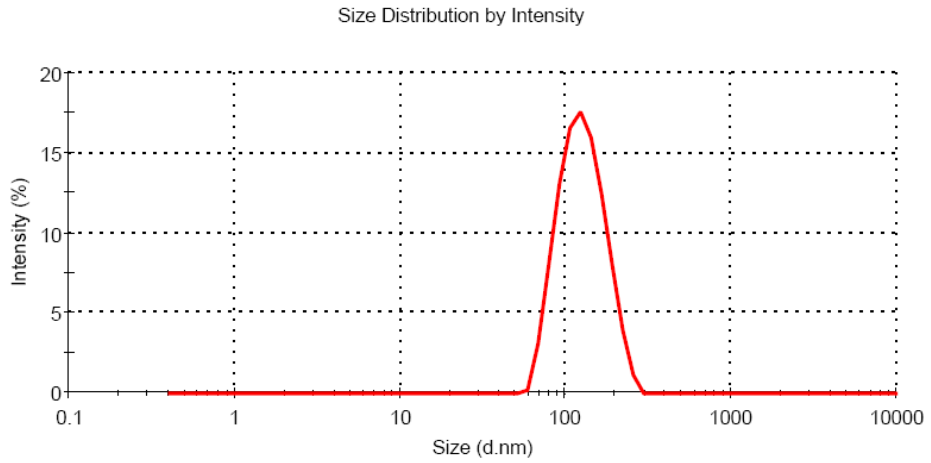

B

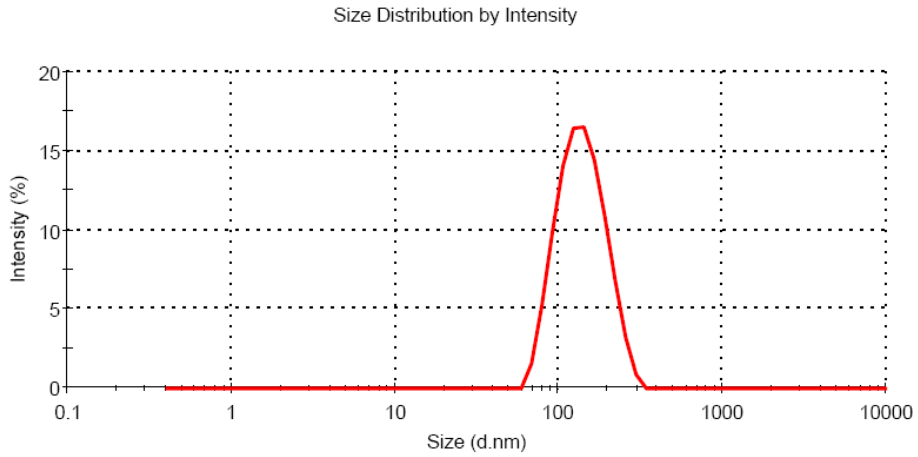

Figure 1: Polydispersity index (PDI) and size distribution of liposomes as determined by dynamic light scattering analysis. A, The size distribution for non-targeted liposomes was found to have a mean size of 118 nm and PDI of 0.110. B, The size distribution for targeted liposomes had mean size of 129 nm with PDI of 0.101. Average zeta potentials for both were -29 mV.

In Vitro Experiments

Cell Culture

Mouse microglia-derived BV-2 cells were provided by Dr. Steven Levison (New Jersey Medical School). The murine BV-2 cell line was original generated by Blasi et al (1990) and exhibits phenotypic and functional properties of reactive microglial cells. Cells were maintained in Dulbecco's Modified Eagle Medium supplemented with 10% heat inactivated Fetal Bovine Serum and 1% Penicillin-Streptomycin at 37 °C in a 5% CO_2 atmosphere. All cell culture materials were purchased from Invitrogen (Carlsbad, CA).

Cell Uptake Study

An uptake study with BV-2 cells was performed to investigate the ability of the cells to internalize the liposomes. For this experiment, targeted liposomes were labeled with rhodamine (Avanti Lipids, Alabaster, AL) at 1 molar percent. BV-2 cells were cultivated on a chamber slide for 24 hours at a starting density of 10,000 cells each. The rhodamine-labeled liposomes were added to the cells at 200 μmol/ml and incubated at 37°C for 120 minutes. Media was removed from the chambers and the slide fixed with 4% paraformaldehyde. The cells were stained with 4,6-diamidino-2-phenylindole (DAPI) for visualization of the nuclei, and then washed three times with PBS to end exposure to adherent liposomes. Slides were then viewed under fluorescent microscope.

Flow Cytometry Assay

Flow cytometry was used to measure total intracellular liposome fluorescence, which is an indirect measure of intracellular drug content. This allows for relative quantification of drug accumulation between targeted and non-targeted liposomes, and thus specificity to the pathological site. Fresh batches of targeted and non-targeted liposomes were synthesized with rhodamine at 1 molar percent. Cells ($1x10^6$) were exposed to 200 μmol/ml media of either targeted or non-targeted liposomes or the equivalent volume of PBS and incubated at 37^oC for 120 minutes. The cells were then centrifuged (5 minutes, 1000 rpm) and washed with PBS twice to remove any remaining liposomes. Following the last centrifugation, cells were resuspended in 1 ml PBS for flow cytometry assay.

The intracellular accumulation of rhodamine-labeled liposomes was evaluated using a fluorescence activated cell analyzer (FACSII; Becton Dickinson, Sparks, MD). A single 15-mW argon ion laser beam (570 nm) was used to excite the fluorescence of rhodamine with a total of 10,000 cells analyzed for each intensity histogram. The flow cytometry experiment was repeated three times for each treatment condition.

Cytokine enzyme-linked immunosorbent assays (ELISAs)

BV-2 cells were grown to confluency in 24-well cell culture plates (BD Biosciences, San Jose, CA) with 0.5 ml media. The cells were activated with 10 ng/ml IFN-γ (Sigma, St. Louis, MO) and simultaneously treated with 40 μM minocycline (Sigma, St. Louis, MO) contained in targeted liposomes or non-targeted liposomes, or as free drug. Cells activated with IFN-γ and receiving no treatment served as positive controls for activation, while BV-2 cells receiving media alone served as true controls.

The concentration of minocycline was chosen based on previous *in vitro* studies (Kremlev et al, 2004; Nikodemova et al, 2006), as well as our own studies involving graded minocycline concentrations (data not shown). After 24-hour incubation at 37^{o}C, the supernatant was collected for each condition and TNF-α was measured using a standard mouse ELISA kit (R&D Systems, Minneapolis, MN) according to the manufacturer's protocol. Plates were then washed with Hank's Balanced Salt Solution and the cells lysed with RIPA buffer for protein quantification with a Bio-Rad DC Protein Assay (Bio-Rad Laboratories, Hercules, CA).

In Vivo Experiments

Animals

Transgenic mice with mutation B6SJL-Tg(SOD1-G93A)1Gur/J were purchased from Jackson Laboratory (Bar Harbor, ME). These mice overexpress mutant human SOD1^{G93A} and develop ALS symptoms (age-related spinal neuron degeneration, muscle atrophy, and shortened lifespan) at approximately 90 days of age. Treatment with minocycline containing liposomes began at 70 days, wherein the animals were fitted with an intracerebroventricular catheter and osmotic pump to continuously deliver minocycline to the lateral ventricle. The experiments were conducted in accordance with Institutional Animal Care and Use Committee (IACUC) guidelines of Pennsylvania State University.

Implant of Osmotic Pump

An implanted osmotic pump (Alzet, Cupertino, CA) was used to continuously deliver liposomes at a rate of 0.25 µl per hour for 28 days. The final concentration of minocycline for delivery was 2 mg/200 µl. Mice were implanted with the pump under general anesthesia (70 mg/kg ketamine and 14 mg/kg xylazine, injected intramuscularly), wherein the animal's scalp was shaved and cleaned and a burr hole (approximately the size of a 25-gauge needle) made at +1.0 mm lateral and –0.46 mm caudal to Bregma. A cannula of depth 2.0 mm was fixed to the animal's skull with cyanoacrylate adhesive. Cannula placement was confirmed following disease endpoint on brains perfused and fixed in 4% paraformadehyde. The osmotic pump was placed in a subcutaneous pocket on the animal's back, with a subcutaneous catheter connecting the pump to the cannula. After placement of the pump, catheter, and cannula, the scalp incision was closed with interrupted sutures. This surgery occurred at 70 days of age. After four weeks, the pump is replaced with a new pump containing fresh liposomes. After this, the pumps were left in place to minimize stress to the animals.

Motor Performance and Endpoint

Motor performance was evaluated three times a week using a rotarod apparatus rotating at 15 rpm (Figure 2). Mice were habituated to the rotarod over the course of a five day learning period beginning at 8 weeks of age. A mouse was considered to fail the test when it could not stay on the rotating rod for >1 s.e.m. of the number of times it fell during the pre-symptomatic phase (Van Den Bosch et al, 2002). The endpoint of the study is defined by when a mouse cannot right itself in 30 seconds when placed on its

side or the inability to maintain basic grooming and feeding behavior (Zhang et al, 2003; Gurney et al, 1996).

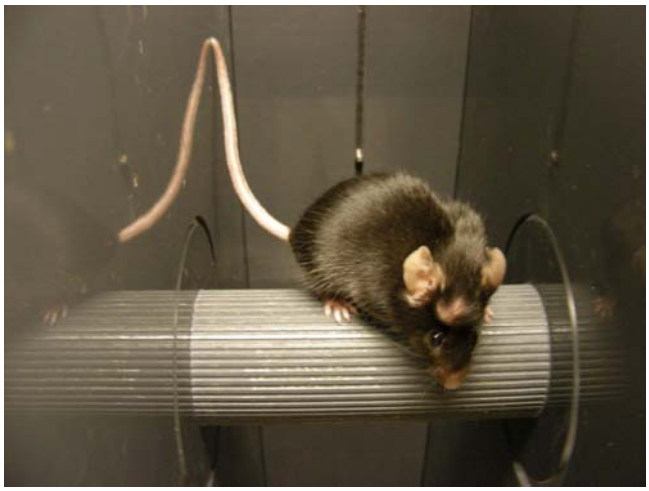

Figure 2: SOD1^{G93A} mouse on rotarod apparatus. The intracerebroventricular cannula that delivers the drug treatment can be seen subcutaneously on the animals scalp. Mice were tested three times a week on the rotarod apparatus to assess motor performance.

Data Analysis and Statistics

Statistical significance was determined by one-way ANOVA with Tukey's post hoc test. For Kaplan-Meier survival plots, statistical significance was determined using a logrank test (GraphPad Prism 4.03). Significance for all analyses is defined as $p<0.05$.

RESULTS

In Vitro Results

In order to establish proof of concept for our studies we first demonstrated the relative *in vitro* uptake of the targeted and untargeted liposomes into cells. As such, the cellular uptake and accumulation was assessed with fluorescent microscopy and flow cytometry using the BV-2 cell line. Figure 3 illustrates the uptake of targeted liposomes into BV-2 cells, as demonstrated by the red fluorescent rhodamine being clearly visible within the cell.

A

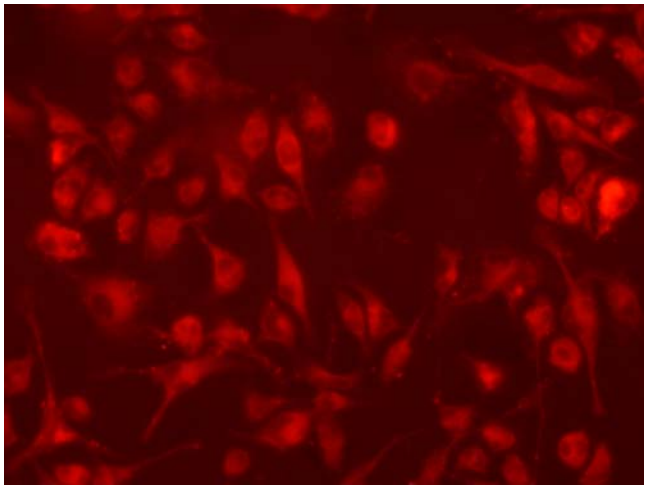

B

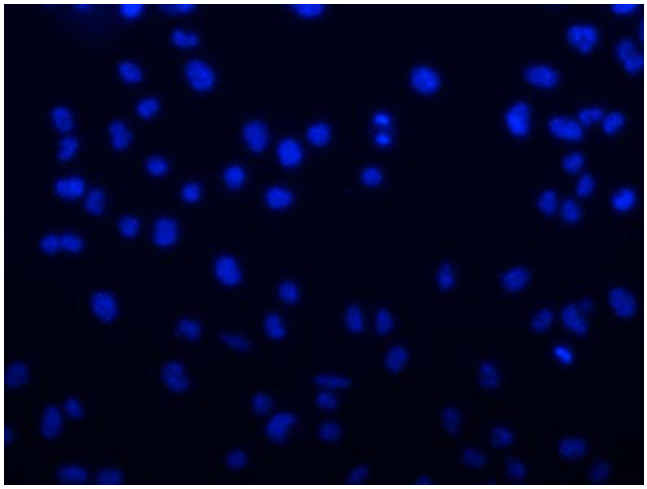

C

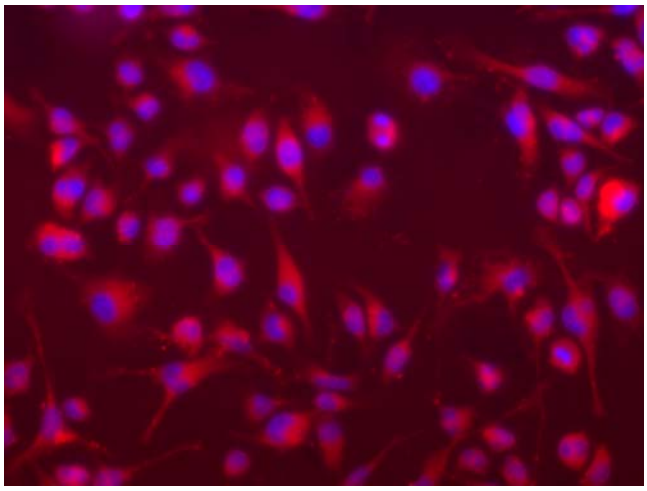

Figure 3: Uptake of LPS-conjugated rhodamine-labeled liposomes into mouse microglia-derived BV-2 cells. The cells were exposed to liposomes for 2 hours. **A**, Uptake is clearly visible by the fluorescent image revealing rhodamine-containing microglia. **B**, Cells were also treated with 4,6-diamidino-2-phenylindole (DAPI) nuclear staining. **C**, Overlay of rhodamine (red) and DAPI (blue) staining.

The flow cytometry analysis revealed an increase of intracellular cell fluorescence in targeted liposome-treated cells as compared to cells treated with non-targeted liposomes for the same duration of time (Figure 4A). This is evidenced by a right shift in the flow cytometric histogram and the correlating mean fluorescent intensity units. Normalization of the signals to endogenous fluorescence resulted in a 3.07 and 3.95 fold fluorescent change in targeted versus non-targeted conditions, respectively (Figure 4B). This represents a 29% increase ($p < 0.05$), indicating an accumulation of the liposomes, in the targeted versus non-targeted liposomal conditions.

A

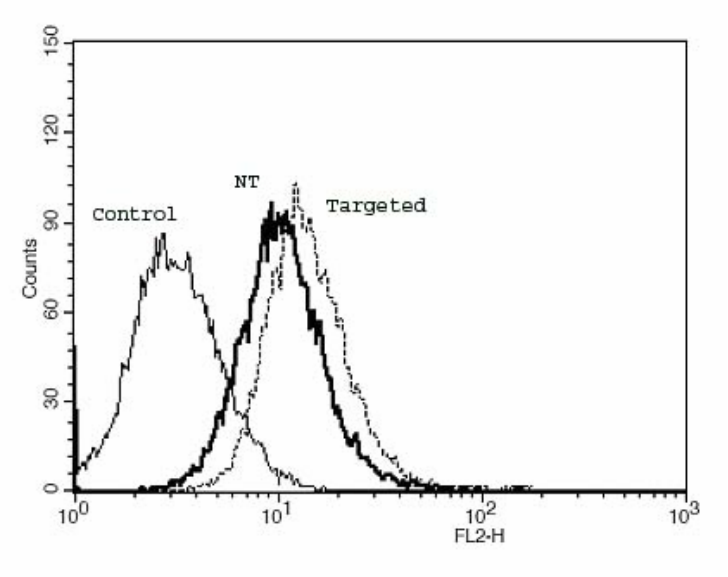

B

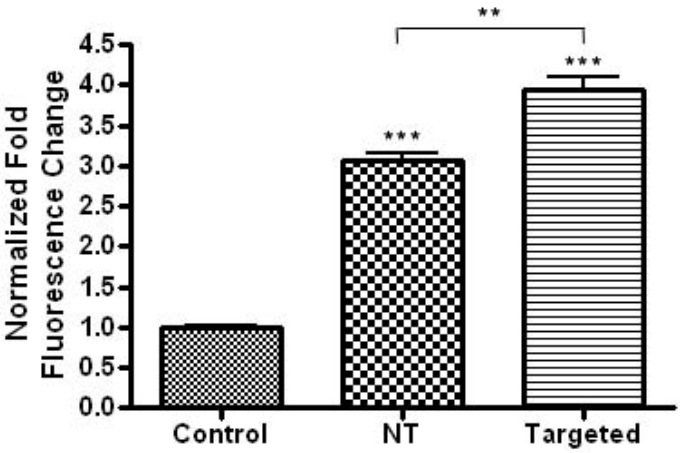

Figure 4: Flow cytometric analysis of liposome accumulation in BV-2 cells. **A**, representative overlay of the fluorescence intensity of BV-2 cells treated with targeted versus non-targeted (NT) liposomes. Targeted liposomes with the conjugated LPS moiety resulted in a right shift of the curve, hence an increased accumulation of liposomes over a 2 hour exposure. **B**, After normalization of the endogenous fluorescent signal (control), analysis reveals a significant increase ($p<0.01$) of 29% in the fluorescent change from non-targeted to targeted treatments. Each condition has n=3, and was run in duplicate. The control conditions are BV-2 cells devoid of treatment.

ELISA kits were utilized to measure the concentrations of TNF-α from activated and non-activated BV-2 cells under various treatment conditions. Cells exposed to IFN-γ for 48 hours had a significant increase ($p<0.001$) in TNF-α secretion, as shown in Figure 5A. Levels of TNF-α were attenuated when activation was coupled with a treatment condition. This attenuation was statistically significant for minocycline-encapsulated non-targeted liposomes and free minocycline with a p-value < 0.001, and for minocycline-encapsulated targeted liposomes with a p-value < 0.01. There was no statistically significant difference ($p>0.05$) between targeted liposome and free minocycline conditions; however, levels of TNF-α were significantly decreased with non-targeted versus targeted liposomes. The relative level of TNF-α inhibition from the positive control can be seen in Figure 5B. The ability of minocycline to inhibit TNF-α secretion as a function of different delivery modalities was 22.3% for targeted liposomes, 39.1 % for NT liposomes, and 34.9% for free minocycline.

A

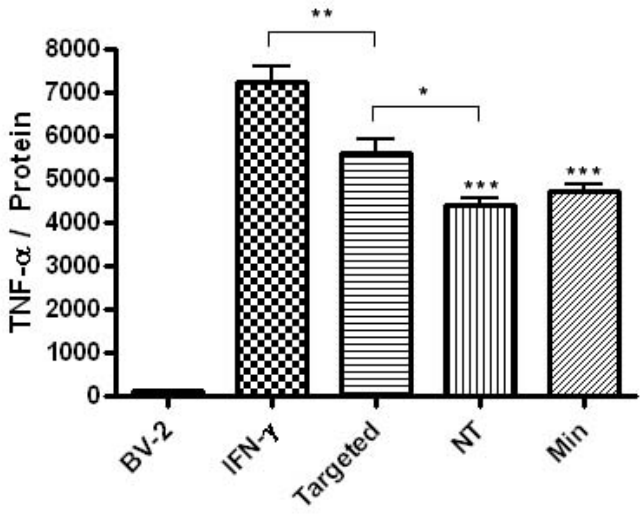

B

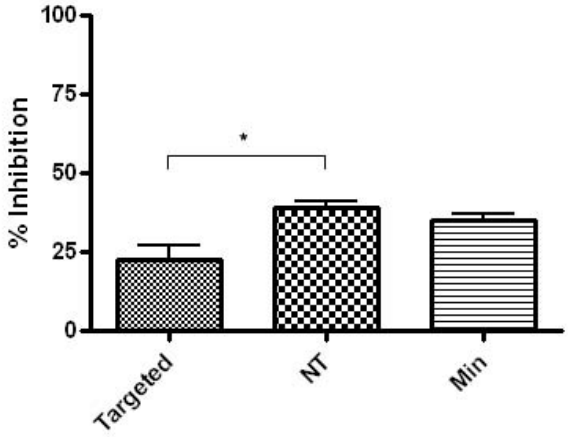

Figure 5: Quantification of TNF-α by standard mouse ELISA kit.
A, BV-2 cells were exposed to 10 ng/ml IFN-γ in media and simultaneously treated with 40 μM minocycline encapsulated in targeted or non-targeted (NT) liposomes, or as free drug (Min). Exposure duration was 48 hours. The control group consisted of BV-2 cells without activation or treatment condition. There was a significant decrease ($p<0.001$ for NT and Min, $p<0.01$ for targeted) in TNF-α levels with all three treatment groups as compared to activated cells alone. All conditions were run in duplicate with n=3. **B,** The relative TNF-α inhibition as compared to activated cells receiving no treatment was 22.3%, 39.1%, and 34.9% for targeted, NT, and Min respectively.

In Vivo Results

$SOD1^{G93A}$ mice treated with non-targeted minocycline liposomes prior to disease onset significantly extended time ($p<0.01$) to rotarod failure and disease endpoints as compared to mice receiving no treatment. Conversely, there was only a significant latency to disease endpoint, and not rotarod failure, seen with the targeted liposome-treated group. As seen in Table 1, the mean age for rotarod failure in the untreated control mice was 103.0 days, whereas the mean age for the targeted minocycline

liposome group was 111.1 days ($p>0.05$) and the non-targeted group was 116.0 days ($p<0.01$). Moreover, survival was significantly increased ($p<0.05$) to 133.0 and 135.0 days with both targeted and NT therapies, respectively, compared to 124.3 days in the control group. These delays represent an increase of 8% (targeted group) and 13% (non-targeted group) for age at rotarod failure, and 7% and 9% latency to disease endpoint, respectively. Likewise, the Kaplan-Meier plot of the cumulative probability of rotarod failure displays a clear and statistically significant difference (logrank test, $p<0.05$) between control and non-targeted liposome groups (Figure 6A). The survival plot of disease endpoints for both targeted and non-targeted treatment groups shows a statistically significant difference (logrank test, $p<0.05$) as compared to controls (Figure 6B).

	Rotarod Failure (Days)	Endpoint (Days)
Control (n=7)	103.0 $\pm$ 2.1	124.3 $\pm$ 1.3
Targeted (n=7)	111.1 $\pm$ 2.9	133.0 $\pm$ 3.1 *
NT (n=6)	116.8 $\pm$ 2.4 **	135.0 $\pm$ 1.8 *

Table 1: Mean age at time of rotarod failure and endpoint stages. Data are expressed as mean $\pm$ s.e.m. Rotarod failure was defined as the point in which a mouse could not stay on the rotating rod for >1 s.e.m. of the number of times it fell during the pre-symptomatic training phase. Mice were tested three times a week at 15 rpm. Disease endpoint was reached when the mouse could not right itself in 30 seconds when placed on its side. * $p<0.05$, ** $p<0.01$

A

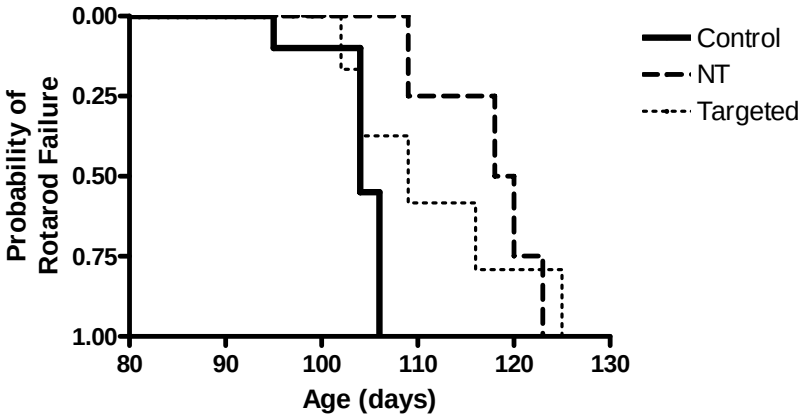

B

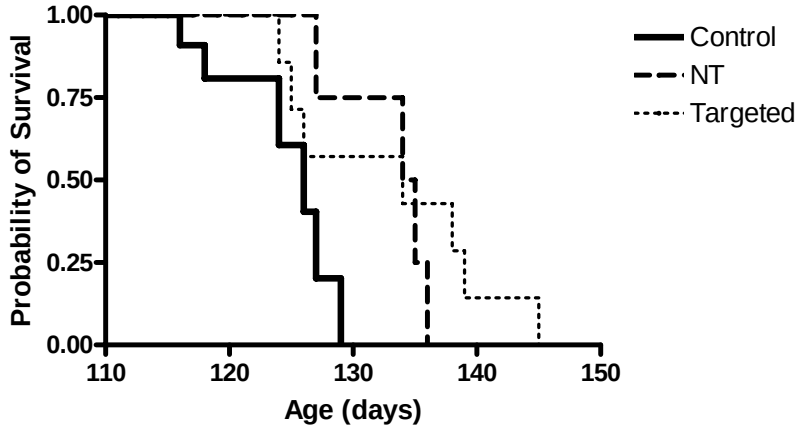

Figure 6: Kaplan-Meier plots of the cumulative probability of rotarod failure and death. **A**, The therapeutic effect of non-targeted liposomes on motor performance of $SOD1^{G93A}$ mice as compared to controls can be seen by the right shift in the survival curve. Analysis with a logrank test reveals a significant shift ($p<0.05$) in the curve of the non-targeted liposome treated group. The right shift for the targeted liposome group did not reach statistical significance ($p>0.05$). **B**, Analysis of the age at disease endpoint for $SOD1^{G93A}$ mice receiving both targeted and NT liposome treatments revealed a significant difference ($p<0.05$) in age at death compared to that of controls for both treatment groups.

DISCUSSION

The present study was designed to deliver nanovesicles containing a therapeutic agent via intracerebroventricular infusion. The purpose of this study was two-fold: (i) to determine if the intracerebroventicular approach had therapeutic efficacy and (ii) to test the hypothesis that an LPS-conjugated targeting moiety would be more effective than non-targeted liposomes. The approach in this not only has the potential to contribute to the understanding of underlying disease mechanisms but also to develop treatment options. First, our data showed the uptake of targeted nanovesicles into BV-2 cells *in vitro* through visualization of rhodamine by fluorescence microscopy. In addition, flow cytometric analyses revealed that placing minocycline within targeted liposomes resulted in a significant, 29% increase in uptake by BV-2 cells as compared to non-targeted liposomes exposed for the same duration of time. These data reveal that nanovesicles encapsulating minocycline can be taken up by microglia and that targeting the nanovesicles via the TLR4/LPS interaction increases the efficiency of uptake. Previous studies have shown that TLR4 is not expressed on neurons, astrocytes, or oligodendrocytes (Hoshino et al, 1999; Lehnardt et al, 2002), thus TLR4 meets the criteria for selective targeting to microglia.

Next, we demonstrated the ability of our liposome treatment to decrease expression of the inflammation marker TNF-α in an ELISA experiment. To this end, both targeted and non-targeted liposomes resulted in decreased TNF-α secretion in activated BV-2 microglial cells as compared to activated cells receiving no treatment. Further, these effects (level of TNF-α secretion) with the liposome encapsulated

minocycline were shown to be comparable to that of free minocycline. Thus the neuroprotective effects of minocycline delivered via liposomes was not compromised by delivering the drug encapsulated in the liposomes. There is a significant difference in TNF-α secretion between the targeted and non-targeted minocycline liposomes with *in vitro* BV-2 cultures. The non-targeted liposomes had a greater effect than the targeted in terms of reducing the levels of TNF-α released by the BV-2 cells. Therefore, there does not appear to be any corollary between speed of uptake and the effect on cytokine secretion. Alternatively, targeting the TLR4/LPS complex may have attenuated the efficacy of the minocycline by activating the TLR4 signaling pathway, which might also explain the increased uptake of targeted liposomes.

The potential therapeutic efficacy of the targeted and non-targeted minocycline liposomes was tested in $SOD1^{G93A}$ mice. Our data demonstrate that the non-targeted nanovesicles significantly increased the latency to rotarod failure and both targeted and non-targeted nanovesicles significantly delayed disease endpoints. While there was an increase in the mean age of rotarod failure for the targeted liposome-treated versus the control groups, the difference (8%) was not statistically significant. The data for the targeted liposomes is consistent with a recent study which demonstrated that diminishing the expression of mutant SOD1 in microglia has little effect on the early disease phase but sharply slowed later disease progression. These data suggest that onset and progression are thus represented by distinct disease phases that can be characterized by mutant SOD1 action within different CNS cell types (Boillée et al, 2006; Miller et al, 2006) and raise the possibility that targeted and non-targeted liposomes may be used effectively to combat different stages of the disease. Taken together, the findings suggest a strong potential for therapeutic intervention via intracerebroventricular injection of

nanovesicles to halt microglia activation (via effective targeting systems) and thereby slow the kinetics of disease progression.

Comparative analysis of the present study to previous studies involving minocycline therapy with $SOD1^{G93A}$ mice displays a similar effect in the latency to disease endpoints (Table 2). However, important to this analysis is the improved efficacy in terms of the daily administered dosage. That is, ICV delivery requires less dosage with the same relative effect because of the local drug action. Rotarod failure and disease onset on not listed in the table due to ambivalent definitions of disease stages across studies (i.e. researchers use different rotarod speeds, durations, testing frequencies, and identifying criteria).

SOD1-G93A	Dose; Age at Start of Treatment	Disease Endpoint	Latency (days)	Latency (%)	Reference
Control	N/A	125.6	-	-	Zhu et al, 2002
Treated	10 mg/kg, i.p., daily; 5 weeks	136.8	11.2	8.9%	
Control	N/A	126.3	-	-	Zhang et al, 2003
Treated	22 mg/kg, i.p., daily; 4 weeks	142.2	15.9	12.6%	
Control	N/A	130.3	-	-	Van Den Bosch et al, 2002
Treated	25 mg/kg, i.p., daily; 10 weeks	142.9	12.6	9.7%	
Treated	50 mg/kg, i.p., daily; 10 weeks	150.9	20.6	15.8%	
Control	N/A	124.3	-	-	Present Study
Treated (Targeted Liposomes)	~4 mg/kg/day, i.c.v., continuously; 10 weeks	133.0	8.7	7.0%	
Treated (NT Liposomes)	~4 mg/kg/day, i.c.v., continuously; 10 weeks	135.0	10.7	8.6%	

Table 2: Comparison of present study with previous $SOD1^{G93A}$ mouse models and minocycline therapy. Disease endpoints are expressed as the mean for each respective condition. Note that the present study utilizes the lowest dose of minocycline per diem and begins treatment at 10 weeks, and yet yields comparable efficacy compared to previous studies.

Investigation into novel therapies and drug delivery systems is vitally important, given that the current treatment for ALS includes only one FDA approved drug (riluzole) that has exhibited modest and variable efficacy (Bensimon et al, 1994; Lacomblez et al, 1996). No other drug has proven effective in the decade since its introduction, and thus it is apparent that relatively little is known about the molecular mechanisms modulating the disease. Nonetheless, the present study demonstrates the selective targeting ability through the TLR4/LPS complex and the consequent impact of delivering anti-inflammatory drugs to microglia. Importantly, the findings suggests that targeting putative therapeutic agents to microglia may be a viable strategy in slowing disease progression in clinical practice where treatment will naturally follow onset of symptoms. Given the therapeutic efficacy of non-targeted liposomes in this study, the data suggest that uptake of minocycline by neurons and astrocytes had an effect on disease progression that was different from specifically targeting microglia. This may be indicative of a role of oxidative stress from reactive astrocytes on early disease progression and the subsequent anti-oxidant action of minocycline to reduce levels of reactive oxygen species (Floyd, 1999; Kraus et al, 2005). In addition, it has been shown that the proinflammatory factors secreted by microglia downregulate glutamate transporters in astrocytes resulting in insufficient clearance of glutamate and increased excitotoxicity to motor neurons (Rothstein et al, 1995; Tilleux and Hermans, 2007) - an interaction that may explain why non-selective drug administration to all cell types delayed both onset of symptoms and endpoint stages. Nonetheless, the present study showed that targeting microglia may be an effective strategy in slowing later disease progression in ALS. This finding could potentially have a significant impact on the

broader class of neurodegenerative disease - essentially all neurodegenerative conditions involve the activation of microglia and subsequent apoptosis of neuronal cells.

REFERENCES

Alexianu ME, Kozovska M, Appel SH. (2001) Immune reactivity in a mouse model of familial ALS correlates with disease progression, *Neurology*; 57(7): 1282-1289.

Arvin KL, Han BH, Du Y, Lin SZ, Paul SM, Holtzman DM. (2002) Minocycline markedly protects the neonatal brain against hypoxic-ischemic injury, *Annals of Neurology*; 52(1): 54–61.

Bangham AD. (1972) Lipid bilayers and biomembranes, *Annual Review of Biochemistry*; 41:753-776.

Bangham AD and Horne RW. (1964) Negative staining of phospholipids and thief structural modification by surface-active agents as observed in the electron microscope, *Journal of Molecular Biology*; 8:660-668.

Bensimon G, Lacomblez L, Meininger V. (1994) A controlled trial of riluzole in amyotrophic lateral sclerosis. ALS/Riluzole Study Group, *New England Journal of Medicine*; 330(9): 585-591.

Blasi E, Barluzzi R, Bocchini V, Mazzolla R, Bistoni F. (1990) Immortalization of murine microglial cells by a v-raf/v-myc carrying retrovirus, *Journal of Neuroimmunology*; 27(2-3):229-237.

Boillée S, Yamanaka K, Lobsiger CS, Copeland NG, Jenkins NA, Kassiotis G, Kollias G, Cleveland DW. (2006) Onset and progression in inherited ALS determined by motor neurons and microglia, *Science*; 312(5778):1389-1392.

Bruijn LI, Houseweart MK, Kato S, Anderson KL, Anderson SD, Ohama E, Reaume AG, Scott RW, Cleveland DW. (1998) Aggregation and motor neuron toxicity of an ALS-linked SOD1 mutant independent from wild-type SOD1, *Science*; 281(5384):1851-1854.

Brundula V, Rewcastle NB, Metz LM, Bernard CC, Yong VW. (2002) Targeting leukocyte MMPs and transmigration: minocycline as a potential therapy for multiple sclerosis, *Brain*; 125(pt 6); 1297-1308.

Charcot M and Joffrey A (1869) Deux cas d'atrophie musculaire progressive avec lesions de la substance grise et desfarsilaux anterior-latéraux de la moelle épinière. *Archives Physiologie Normale et Pathologié*; 2:354–367:629–649:744–760.

Chen M, Ona VO, Li M, Ferrante RJ, Fink KB, Zhu S, Bian J, Guo L, Farrell LA, Hersch SM, Hobbs W, Vonsattel JP, Cha JH, Friedlander RM. (2000) Minocycline inhibits caspase-1 and caspase-3 expression and delays mortality in a transgenic mouse model of Huntington disease, *Nature Medicine*, 6(7): 797-801.

Chonn A, Cullis PR, Devine DV. (1991) The role of surface charge in the activation of the classical and alternative pathways of complement by liposomes, *Journal of Immunology*; 146(12):4234-4241.
Chow JC, Young DW, Golenbock DT, Christ WJ, Gusovsky F. (1999) Toll-like receptor-4 mediates lipopolysaccharide-induced signal transduction. *Journal of Biological Chemistry*; 274(16):10689-10692.

del Rio-Hortega P. (1958) Studies on the centrosome of nerve cells and neuroglia of vertebrates; normal & abnormal forms, *Archivos de histología normal y patológica*; 7(2):77-114.

Du Y, Ma Z, Lin S, Dodel RC, Gao F, Bales KR, Triarhou LC, Chernet E, Perry KW, Nelson DL, Luecke S, Phebus LA, Bymaster FP, Paul SM. (2001) Minocycline prevents nigrostriatal dopaminergic neurodegeneration in the MPTP model of Parkinson's disease, *Proceedings of the National Academy of Sciences USA*; 98(25): 14669-14674.

Floyd RA. (1999) Antioxidants, oxidative stress, and degenerative neurological disorders. *Proceedings of the Society for Experimental Biology and Medicine*; 222(3):236-45.

Gabizon A, Shmeeda H, Barenholz Y. (2003) Pharmacokinetics of pegylated liposomal Doxorubicin: review of animal and human studies, *Clinical Pharmacokinetics*; 42(5):419-436.

Gordon PH, Moore DH, Miller RG, Florence JM, Verheijde JL, Doorish C, Hilton JF, Spitalny GM, MacArthur RB, Mitsumoto H, Neville HE, Boylan K, Mozaffar T, Belsh JM, Ravits J, Bedlack RS, Graves MC, McCluskey LF, Barohn RJ, Tandan R; Western ALS Study Group. (2007) Efficacy of minocycline in patients with amyotrophic lateral sclerosis: a phase III randomised trial, *Lancet Neurology*; 6(12): 1045-1053.

Gregoriadis G, Wills EJ, Swain CP, Tavill AS. (1974) Drug-carrier potential of liposomes in cancer chemotherapy, *Lancet*, 1(7870):1313-1316.

Gubbay SS, Kahana E, Zilber N, Cooper G, Pintov S, Leibowitz Y. (1985) Amyotrophic lateral sclerosis. A study of its presentation and prognosis, *Journal of Neurology*; 232(5):295-300.

Gurney ME, Cutting FB, Zhai P, Doble A, Taylor CP, Andrus PK, Hall ED. (1996) Benefit of vitamin E, riluzole, and gabapentin in a transgenic model of familial amyotrophic lateral sclerosis, *Annals of Neurology*; 39(2):147-157.

Gurney ME, Pu H, Chiu AY, Dal Canto MC, Polchow CY, Alexander DD, Caliendo J, Hentati A, Kwon YW, Deng HX, et al. (1994) Motor neuron degeneration in mice that express a human Cu,Zn superoxide dismutase mutation, *Science*; 264(5166):1772-5.

Hashizume H, Baluk P, Morikawa S, McLean JW, Thurston G, Roberge S, Jain RK, McDonald DM. (2000) Openings between defective endothelial cells explain tumor vessel leakiness, *American Journal of Pathology*; 156(4):1363-1380.

He Y, Appel S, Le W. (2001) Minocycline inhibits microglial activation and protects nigral cells after 6-hydroxydopamine injection into mouse striatum, *Brain Research*, 909(1-2): 187-193.

Hensley K, Fedynyshyn J, Ferrell S, Floyd RA, Gordon B, Grammas P, Hamdheydari L, Mhatre M, Mou S, Pye QN, Stewart C, West M, West S, Williamson KS. (2003) Message and protein-level elevation of tumor necrosis factor alpha (TNF alpha) and TNF alpha-modulating cytokines in spinal cords of the G93A-SOD1 mouse model for amyotrophic lateral sclerosis, *Neurobiology of Disease*, 14(1):74-80.

Hoshino K, Takeuchi O, Kawai T, Sanjo H, Ogawa T, Takeda Y, Takeda K, Akira S. (1999) Cutting edge: Toll-like receptor 4 (TLR4)-deficient mice are hyporesponsive to lipopolysaccharide: evidence for TLR4 as the Lps gene product, *Journal of Immunology*; 162(7):3749-3752.

Johnson SM, Bangham AD, Hill MW, Korn ED. (1971) Single bilayer liposomes, *Biochimica et biophysica acta*; 233(3):820-826.

Kawamata T, Akiyama H, Yamada T, McGeer PL. (1992) Immunologic reactions in amyotrophic lateral sclerosis brain and spinal cord tissue, *American Journal of Pathology*; 140(3): 691-707.

Kraus RL, Pasieczny R, Lariosa-Willingham K, Turner MS, Jiang A, Trauger JW. (2005) Antioxidant properties of minocycline: neuroprotection in an oxidative stress assay and direct radical-scavenging activity, *Journal of Neurochemistry*; 94(3):819-827.

Kremlev SG, Roberts RL, Palmer C. (2004) Differential expression of chemokines and chemokine receptors during microglial activation and inhibition, *Journal of Neuroimmunology*; 149(1-2):1-9.

Kreutzberg GW. (1996) Microglia: a sensor for pathological events in the CNS, *Trends in Neuroscience*; 19(8):312-318.

Lacomblez L, Bensimon G, Leigh PN, Guillet P, Meininger V. (1996) Dose-ranging study of riluzole in amyotrophic lateral sclerosis. Amyotrophic Lateral Sclerosis/Riluzole Study Group II, *Lancet*; 347(9013): 1425-1431.

Lehnardt S, Massillon L, Follett P, Jensen FE, Ratan R, Rosenberg PA, Volpe JJ, Vartanian T. (2003) Activation of innate immunity in the CNS triggers neurodegeneration through a Toll-like receptor 4-dependent pathway, *Proceedings of the National Academy of Sciences USA*; 100(14):8514-8519.

Lehnardt S, Lachance C, Patrizi S, Lefebvre S, Follett PL, Jensen FE, Rosenberg PA, Volpe JJ, Vartanian T. (2002) The toll-like receptor TLR4 is necessary for lipopolysaccharide-induced oligodendrocyte injury in the CNS, *Journal of Neuroscience*; 22(7):2478-2486.

Li L, Lu J, Tay SS, Moochhala SM, He BP. (2007) The function of microglia, either neuroprotection or neurotoxicity, is determined by the equilibrium among factors released from activated microglia in vitro, *Brain Research*; 1159:8-17.

Madhankumar AB, Slagle-Webb B, Mintz A, Sheehan JM, Connor JR. (2006) Interleukin-13 receptor-targeted nanovesicles are a potential therapy for glioblastoma multiforme, *Molecular Cancer Therapeutics*; 5(12): 3162-3169.

McGeer PL, Itagaki S, Boyes BE, McGeer EG (1988) Reactive microglia are positive for HLA-DR in the substantia nigra of Parkinson's and Alzheimer's disease brains, Neurology; 38(8):1285-1291.

Miller TM, Kim SH, Yamanaka K, Hester M, Umapathi P, Arnson H, Rizo L, Mendell JR, Gage FH, Cleveland DW, Kaspar BK. (2006) Gene transfer demonstrates that muscle is not a primary target for non-cell-autonomous toxicity in familial amyotrophic lateral sclerosis, *Proceedings of the National Academy of Sciences USA*; 103(51): 19546-19551.

Milligan CE, Cunningham TJ, Levitt P. (1991) Differential immunochemical markers reveal the normal distribution of brain macrophages and microglia in the developing rat brain, *Journal of Comparative Neurology*; 314(1):125-135.

Mintz A, Gibo DM, Madhankumar AB, Debinski W. (2003) Molecular targeting with recombinant cytotoxins of interleukin-13 receptor alpha2-expressing glioma, *Journal of Neurooncology*; 64(1-2): 117-123.

Morgan CG, Thomas EW, Yianni YP. (1983) The use of fluorescence energy transfer to distinguish between poly(ethylene glycol)-induced aggregation and fusion of phospholipid vesicles, *Biochimica et Biophysica Acta*; 728(3):356-362.

Nikodemova M, Duncan ID, Watters JJ. (2006) Minocycline exerts inhibitory effects on multiple mitogen-activated protein kinases and IkappaBalpha degradation in a stimulus-specific manner in microglia, *Journal of Neurochemistry*; 96(2):314-323.

Nguyen MD, D'Aigle T, Gowing G, Julien JP, Rivest S. (2004) Exacerbation of motor neuron disease by chronic stimulation of innate immunity in a mouse model of amyotrophic lateral sclerosis, *Journal of Neuroscience*; 24(6): 1340-1349.

Rahman A, Treat J, Roh JK, Potkul LA, Alvord WG, Forst D, Woolley PV. (1990) A phase I clinical trial and pharmacokinetic evaluation of liposome-encapsulated doxorubicin, *Journal of Clinical Oncology*; 8(6):1093-1100.

Raivich G, Bluethmann H, Kreutzberg GW. (1996) Signaling molecules and neuroglial activation in the injured central nervous system, *Keio Journal of Medicine*; 45(3):239-247.

Reaume AG, Elliott JL, Hoffman EK, Kowall NW, Ferrante RJ, Siwek DF, Wilcox HM, Flood DG, Beal MF, Brown RH Jr, Scott RW, Snider WD. (1996) Motor neurons in Cu/Zn superoxide dismutase-deficient mice develop normally but exhibit enhanced cell death after axonal injury, *Nature Genetics*, 13(1):43-47.

Ringel SP, Murphy JR, Alderson MK, Bryan W, England JD, Miller RG, Petajan JH, Smith SA, Roelofs RI, Ziter F, et al. (1993) The natural history of amyotrophic lateral sclerosis, *Neurology*; 43(7):1316-22.

Rogers J, Luber-Narod J, Styren SD, Civin WH. (1988) Expression of immune system-associated antigens by cells of the human central nervous system: relationship to the pathology of Alzheimer's disease; Neurobiology of Aging, 9(4):339-349.

Rosen DR, Siddique T, Patterson D, Figlewicz DA, Sapp P, Hentati A, Donaldson D, Goto J, O'Regan JP, Deng HX, et al. (1993) Mutations in Cu/Zn superoxide dismutase gene are associated with familial amyotrophic lateral sclerosis, *Nature*; 362(6415): 59-62.

Rothstein JD, Van Kammen M, Levey AI, Martin LJ, Kuncl RW. (1995) Selective loss of glial glutamate transporter GLT-1 in amyotrophic lateral sclerosis. *Annals of Neurology*, 38(1): 73-84.

Rowland LP (2001) How Amyotrophic Lateral Sclerosis Got Its Name: The Clinical-Pathologic Genius of Jean-Martin Charcot, *Archives of Neurology*; 58:512-515.

Sanchez Mejia RO, Ona VO, Li M, Friedlander RM. (2001) Minocycline reduces traumatic brain injury-mediated caspase-1 activation, tissue damage, and neurological dysfunction, *Neurosurgery*; 48(6):1393-1399.

Scott S, Kranz JE, Cole J, Lincecum JM, Thompson K, Kelly N, Bostrom A, Theodoss J, Al-Nakhala BM, Vieira FG, Ramasubbu J, Heywood JA. (2008) Design, power, and interpretation of studies in the standard murine model of ALS, *Amyotrophic Lateral Sclerosis*; 9(1):4-15.

Segal AW, Wills EJ, Richmond JE, Slavin G, Black CD, Gregoriadis G. (1974) Morphological observations on the cellular and subcellular destination of intravenously administered liposomes, *British Journal of Experimental Pathology*; 55(4):320-327.

Vaage J, Donovan D, Uster P, Working P. (1997) Tumour uptake of doxorubicin in polyethylene glycol-coated liposomes and therapeutic effect against a xenografted human pancreatic carcinoma, *British Journal of Cance*r; 75(4):482-486.

van Den Bosch L, Tilkin P, Lemmens G, Robberecht W. (2002) Minocycline delays disease onset and mortality in a transgenic model of ALS, *Neuroreport*; 13(8):1067-1070.

van Rossum D and Hanisch UK. (2004) Microglia, *Metabolic Brain Disorders*; 19(3-4):393-411.

Wang X, Zhu S, Drozda M, Zhang W, Stavrovskaya IG, Cattaneo E, Ferrante RJ, Kristal BS, Friedlander RM. (2003) Minocycline inhibits caspase-independent and -dependent mitochondrial cell death pathways in models of Huntington's disease, *Proceedings of the National Academy of Sciences USA*; 100(18):10483-10487.

Wells JE, Hurlbert RJ, Fehlings MG, Yong VW. (2003) Neuroprotection by minocycline facilitates significant recovery from spinal cord injury in mice, *Brain*; 126(Pt 7): 1628-1637.

Wong PC, Pardo CA, Borchelt DR, Lee MK, Copeland NG, Jenkins NA, Sisodia SS, Cleveland DW, Price DL. (1995) An adverse property of a familial ALS-linked SOD1 mutation causes motor neuron disease characterized by vacuolar degeneration of mitochondria, *Neuron*; 14(6):1105-16.

Worms PM. (2001) The epidemiology of motor neuron diseases: a review of recent studies, *Journal of Neurological Sciences*; 191(1-2):3-9.

Wu DC, Jackson-Lewis V, Vila M, Tieu K, Teismann P, Vadseth C, Choi DK, Ischiropoulos H, Przedborski S. (2002) Blockade of microglial activation is neuroprotective in the 1-methyl-4-phenyl-1,2,3,6-tetrahydropyridine mouse model of Parkinson disease, *Journal of Neuroscience*; 22(5):1763-1771.

Yrjänheikki J, Keinänen R, Pellikka M, Hökfelt T, Koistinaho J. (1998) Tetracyclines inhibit microglial activation and are neuroprotective in global brain ischemia, *Proceedings of the National Academy of Sciences USA*; 95(26): 15769–15774.

Zhang W, Narayanan M, Friedlander RM. (2003) Additive neuroprotective effects of minocycline with creatine in a mouse model of ALS, *Annals of Neurology*; 53(2):267-270.

Zhu S, Stavrovskaya IG, Drozda M, Kim BY, Ona V, Li M, Sarang S, Liu AS, Hartley DM, Wu DC, Gullans S, Ferrante RJ, Przedborski S, Kristal BS, Friedlander RM. (2002) Minocycline inhibits cytochrome c release and delays progression of amyotrophic lateral sclerosis in mice, *Nature*; 417(6884): 74-78.